

See discussions, stats, and author profiles for this publication at: <https://www.researchgate.net/publication/263420423>

# Viscoelastic, surface, and volumetric properties of ionic liquids [BMIM][O<sub>c</sub>SO<sub>4</sub>], [BMIM][PF<sub>6</sub>], and [EMIM][MeSO<sub>3</sub>]

ARTICLE in JOURNAL OF CHEMICAL & ENGINEERING DATA · JANUARY 2014

Impact Factor: 2.04 · DOI: 10.1021/je5000617

CITATION

1

READS

74

## 6 AUTHORS, INCLUDING:



**Manish Pratap Singh**

University of Aberdeen

26 PUBLICATIONS 205 CITATIONS

SEE PROFILE



**Satish Kumar Mandal**

IIT Kharagpur

4 PUBLICATIONS 18 CITATIONS

SEE PROFILE



**Yogendra Lal Verma**

Banaras Hindu University

11 PUBLICATIONS 42 CITATIONS

SEE PROFILE



**Dr. Abhishek Kumar Gupta**

University of Delhi

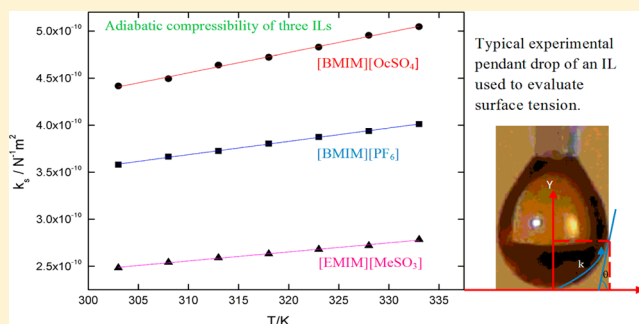
9 PUBLICATIONS 54 CITATIONS

SEE PROFILE

Viscoelastic, Surface, and Volumetric Properties of Ionic Liquids [BMIM][OcSO<sub>4</sub>], [BMIM][PF<sub>6</sub>], and [EMIM][MeSO<sub>3</sub>]Manish Pratap Singh,<sup>†</sup> Satish Kumar Mandal,<sup>‡</sup> Yogendra Lal Verma,<sup>†</sup> Abhishek Kumar Gupta,<sup>†</sup> Rajendra Kumar Singh,<sup>\*,†</sup> and Suresh Chandra<sup>†</sup><sup>†</sup>Department of Physics, Banaras Hindu University, Varanasi 221005, India<sup>‡</sup>Department of Physics and Meteorology, Indian Institute of Technology, Kharagpur 721302, West Bengal, India

## S Supporting Information

**ABSTRACT:** Thermophysical properties viz. surface tension, viscosity, density, and ultrasonic velocity of three ionic liquids 1-butyl-3-methyl imidazolium octyl sulfate [BMIM][OcSO<sub>4</sub>], 1-butyl-3-methyl imidazolium hexafluorophosphate [BMIM][PF<sub>6</sub>], and 1-ethyl-3-methyl imidazolium methanesulfonate [EMIM][MeSO<sub>3</sub>] have been measured in a wide temperature range. Experimental data so obtained have been used to calculate isentropic compressibility, isothermal expansion coefficient, surface entropy, surface enthalpy, and critical temperature (temperature where the distinction between liquid and gas phase vanishes and the surface tension tends to zero). Structure–property correlation for different ILs is also discussed.



## INTRODUCTION

A novel class of ionic materials, termed ionic liquids (ILs), has recently attracted much attention. These are essentially low melting point salts consisting of self-dissociated cations and anions. The combination of large and asymmetric cations like imidazolium or ammonium, phosphonium, pyridinium, etc. with anions like hexafluorophosphate [PF<sub>6</sub>] or [BF<sub>4</sub>], [MeSO<sub>3</sub>], [OcSO<sub>4</sub>], etc. makes them liquid down to unusually low temperatures.<sup>1</sup> ILs have some interesting properties such as extremely low vapor pressure, high thermal and chemical stability, recyclability, wide range of solubility, wide electrochemical window, and liquidus range.<sup>1–8</sup> Due to these exotic properties, ILs have found applications as lubricants,<sup>9</sup> solvents for chemical synthesis,<sup>1</sup> catalysts,<sup>4</sup> as electrolytes for electrochemical devices like batteries<sup>10–12</sup> fuel cells,<sup>13</sup> solar cells,<sup>14</sup> super capacitor,<sup>15</sup> sensors,<sup>16</sup> actuators,<sup>17</sup> electrode deposition,<sup>18</sup> templates for obtaining porous silica matrices, etc.<sup>19–21</sup>

Thermophysical properties (viscosity, density, surface tension, elastic properties, etc.) of ILs are important from its technological and industrial applications point of view. For example, viscosity plays an important role from engineering point of view as it largely affects stirring, flow and lubricating properties; transport properties like diffusion; mixing and pumping processes. Another important thermophysical property is surface tension which affects some important steps related to production process like catalysis, adsorption and extraction. Ultrasonic velocity is an important thermophysical parameter which can give precise information about the processes occurring in the time scale  $10^{-3}$  to  $10^{-10}$  s and is very sensitive to molecular organization and interaction.

Therefore, it can be used as important tool for characterizing materials. Using ultrasonic velocity together with density, viscosity etc. we can evaluate many interesting properties viz. thermal expansion coefficient, isentropic compressibility, attenuation, and relaxation time. Recently, we have reported<sup>22</sup> the correlations between many thermophysical quantities viz. ultrasonic velocity, density, viscosity, and surface tension for three imidazolium based ILs. The correlations developed by us can be used to evaluate the less studied property of ILs viz. speed of sound.

In the present work, we report experimental data on surface tension, fluidity ( $=1/\text{viscosity}$ ), density, and ultrasonic velocity as a function of temperature for three ILs and examine the effect of cation, anion, interactions, and the effect of temperature (since one of the most attractive features of these materials is the wide liquidus range they offer). From these experimental data we have evaluated some important volumetric, surface, and mechanical properties viz. thermal expansion coefficient, molecular volume, surface entropy, surface enthalpy, and isentropic compressibility. The ILs used for the present study are 1-butyl-3-methyl Imidazolium octyl sulfate [BMIM][OcSO<sub>4</sub>], 1-butyl-3-methyl Imidazolium hexafluorophosphate [BMIM][PF<sub>6</sub>], and 1-ethyl-3-methyl Imidazolium methanesulfonate [EMIM][MeSO<sub>3</sub>]. All these ILs are commercially available, out of which [BMIM][PF<sub>6</sub>] is the most studied. However, [BMIM][PF<sub>6</sub>] has been chosen in order to

Received: July 23, 2013

Accepted: June 25, 2014

Published: July 8, 2014

compare our results with numerous available data in the literature. The other two ILs containing octyl sulfate  $[\text{OCSO}_4]$  and methanesulfonate  $[\text{MeSO}_3]$  anions belong to a new generation of fluorine free ILs and are important from the environmental point of view for which limited data are available in the literature.

## EXPERIMENTAL SECTION

**Materials.** The ILs used in this study (1-butyl-3-methyl imidazolium octylsulfate {purity  $\geq 95.0\%$  CAS no. 445473-58-5, water content  $\leq 1.0\%$ }, 1-butyl-3-methyl imidazolium hexa-fluorophosphate {purity  $\geq 98.5\%$  CAS no. 174501-64-5, water content  $\leq 0.02\%$  and halides content  $\leq 10$  mg/kg chloride ( $\text{Cl}^-$ ) and bromide ( $\text{Br}^-$ )}, and 1-ethyl-3-methyl imidazolium methanesulfonate {purity  $\geq 95.0\%$  CAS no. 145022-45-3, water content  $\leq 0.5\%$  and halides content chloride ( $\text{Cl}^-$ ):  $\leq 2\%$ } were procured from Sigma-Aldrich, Germany. The properties of ILs are very sensitive to water content therefore, ILs were dried for 24 h under a vacuum of  $10^{-3}$  Torr to minimize the water content to the extent possible and stored before use in a vacuum desiccator. Also, in order to avoid effect of ambient humidity, ILs were handled under dry nitrogen atmosphere.

**Apparatus and Procedure.** Brookfield DV-III Ultra programmable Rheometer was used for the measurement of viscosity of ILs. The calibration of Rheometer was done with Brookfield standard fluid. CP-40 spindle was used for the measurement of viscosity of the ILs. The deviation in the measurement of the viscosity was about  $\pm 1\%$ . Density,  $\rho$  of the ILs was determined using a pycnometer. The standard uncertainty in the density measurement was about  $2 \cdot 10^{-4} \text{ g} \cdot \text{cm}^{-3}$ . Pycnometer was calibrated using deionized doubly distilled water. For all the measurements of viscosity and density, temperature was controlled by circulating water through an ultra thermostat keeping temperature constant within  $\pm 0.1^\circ \text{C}$  (using a PID controller).

Pendant drop method<sup>22,23</sup> was used for the measurement of the surface tension of the ILs. The experimental arrangement used for the surface tension measurement in this study is described briefly elsewhere.<sup>22</sup> In this method, a drop of IL was generated from a micro syringe and the photographs of the drop have been casted from the 12.1 Mp Sony cyber shot camera. These photographs (for instance an experimental IL pendant drop photograph along with description of meaning of angle  $\theta$ , shape line  $k$ , and axis  $y$  used in eq 1 is shown in Figure 1) have been used to evaluate surface tension ( $\sigma$ ) by solving Laplace's equation for curved interfaces exposed to a gravitational field as

$$\frac{\partial \theta}{\partial k} = \frac{2}{r} - \frac{\Delta \rho g y}{\sigma} - \frac{\sin \theta}{y} \quad (1)$$

where  $r$  is the radius of curvature at a point on the surface having the coordinates  $\theta$  and  $y$ ,  $g$  is the earth's gravitational acceleration, and  $\Delta \rho$  is the density difference of IL and the nitrogen gas. The surface tension  $\sigma$  can be evaluated by solving the differential equation (eq 1) numerically. The standard uncertainty in the surface tension measurement is about  $\pm 0.1 \text{ mN m}^{-1}$ . Due to the sensitivity of ILs to the ambient humidity, all the measurements were carried out in nitrogen environment to avoid frequent drying of ILs during the experiment.

Variable path interferometric technique has been used to measure the ultrasonic velocity at 4 MHz over a wide range of

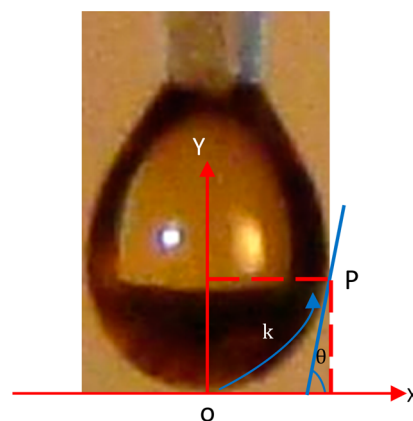


**Figure 1.** Typical experimental IL pendant drop (angle  $\theta$ , shape line  $k$ , and axis  $y$ ) exhibiting the quantities used in Laplace equation.

temperature. In this technique, the IL is placed in a cylindrical sample cell consisting of a double-walled metallic jacket in which inlet and outlet were provided for circulating thermostatic fluid. Sinusoidal RF waves were used to excite an X-cut quartz crystal fitted at the bottom of the cell, which produced longitudinal ultrasonic waves in the liquid medium. These waves get reflected at a metallic reflector. Superposition of incident and reflected (from reflector) ultrasonic waves forms standing wave pattern and nodes and antinodes occur. A sensitive micrometer was fitted with reflector which can be moved up and down with an accuracy of  $1 \mu\text{m}$ . Separation between two consecutive nodes/antinodes is read with the help of a sensitive microammeter in which maxima and minima occur. The separation between these nodes/antinodes is half integral multiple of the wavelength of the ultrasonic wave. A PID controller was used to control the temperature with an accuracy of  $\pm 0.1^\circ \text{C}$ . The estimated standard uncertainty in the measurement of ultrasonic velocity was about  $\pm 0.03\%$ .

All the measurements were carried in the temperature range from (303.0 to 333.0) K and at atmospheric pressure.

## RESULTS AND DISCUSSION

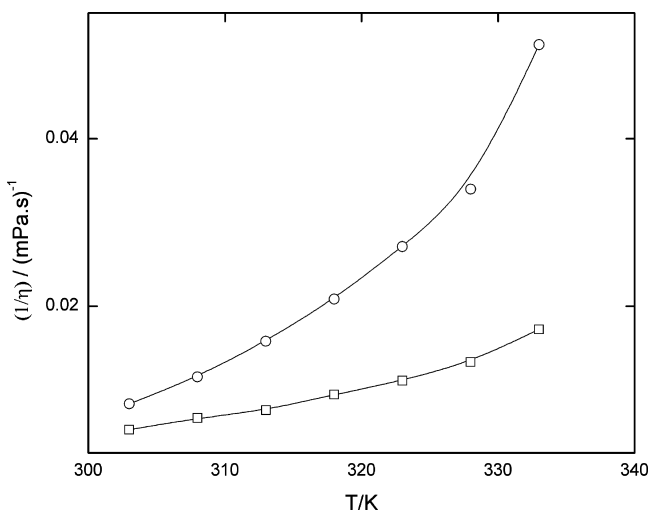
**Viscoelastic Studies. Viscosity (or Fluidity).** Viscosity, an important property of fluids, depends upon molecular geometry, molecular ordering/clustering and intermolecular interactions. Therefore, the study of temperature dependence of viscosity is important. The reciprocal of viscosity ( $1/\eta$ ) termed as "fluidity" and often used in literature. Fluidity has been found to correlate better with the other physical quantities in many cases.<sup>24</sup> Viscosity {or fluidity ( $1/\eta$ )} measured by us for two ILs viz.  $[\text{BMIM}][\text{PF}_6]$  and  $[\text{EMIM}][\text{MeSO}_3]$  is given in Table 1. Figure 2 shows that the nature of the temperature dependent fluidity (and hence viscosity) for two ILs is different possibly because of different molecular structure and molecular interactions. The temperature variation of fluidity can be fitted by the following empirical relation as

$$\left(\frac{1}{\eta}\right)^{0.125} = a + bT \quad (2)$$

where  $a$  and  $b$  are material dependent constants. The solid lines in Figure 2 are the lines calculated from eq 2 by using  $a = -0.28842$ ,  $b = 0.00266$  for  $[\text{BMIM}][\text{PF}_6]$  and  $a = -0.80479$ ,  $b = 0.00447$  for  $[\text{BMIM}][\text{MeSO}_3]$ . Two obvious inferences which can be drawn from Figure 2 are as follows: (a) The

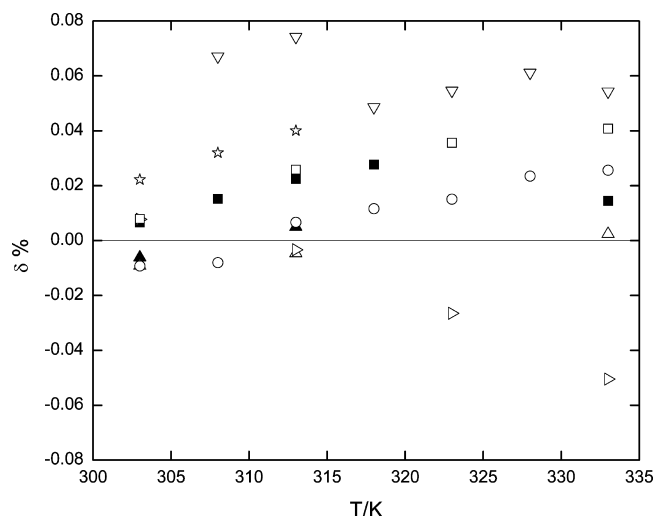
**Table 1.** Viscosity ( $\eta^a$ ) of the ILs from  $T = (303.0 \text{ to } 333.0)$  K at Atmospheric Pressure ( $p = 0.1 \text{ MPa}$ )<sup>b</sup>

$T^c$ K	$\eta^a/\text{mPa}\cdot\text{s}$	
	[BMIM][PF <sub>6</sub> ]	[EMIM][MeSO <sub>3</sub> ]
303.0	190	120
308.0	150	87
313.0	132	63
318.0	106	48
323.0	90	37
328.0	75	29
333.0	58	20

<sup>a</sup> $u(\eta) = \pm 1 \text{ \% mPa}\cdot\text{s}$ . <sup>b</sup>Standard uncertainties. <sup>c</sup> $u(T) = \pm 0.1 \text{ K}$ .**Figure 2.** Temperature dependence of fluidity ( $1/\eta$ ) for  $\square$ , [BMIM][PF<sub>6</sub>] and  $\circ$ , [EMIM][MeSO<sub>3</sub>], – fit from linear eq 2

fluidity of [EMIM][MeSO<sub>3</sub>] is consistently higher than [BMIM][PF<sub>6</sub>]. For viscosity, its opposite is true. This can be understood in terms of relative lengths of the cation chains (i.e., [BMIM] vs [EMIM]) and the symmetry of charge distribution of anions (i.e., [PF<sub>6</sub>] has symmetry while [MeSO<sub>3</sub>] has asymmetry). These two factors may change the intermolecular forces. Lower cation chain length has been reported to give lower viscosity of ILs<sup>25</sup> as found by us for [EMIM]. Further, intermolecular interaction due to asymmetric charge distribution of [MeSO<sub>4</sub>] is likely to be lower and hence viscosity decreases as compared to the symmetric charge distribution of [PF<sub>6</sub>].<sup>26</sup> (b) The fluidity increases with temperature for both the cases but the nature of temperature dependence is different. This can be explained in view of the discussion given above. The viscosity value obtained is a reflection of all the factors described above which are to be taken into account to describe the behavior of this important parameter.<sup>25,26</sup>

Measured viscosity values of [BMIM][PF<sub>6</sub>] and [EMIM][MeSO<sub>3</sub>] are in good agreement with values reported in literature, in the temperature range of the present study. Figure 3 shows the deviations between our ( $1/\eta$ ) values from fitted data and ( $1/\eta$ ) values available in literature. From Figure 3, it can be seen that the maximum deviation for [BMIM][PF<sub>6</sub>] is about 3.8% with respect to Jiqin et al.<sup>27</sup> As expected, the literature data for dried samples are generally close to our values for [BMIM][PF<sub>6</sub>] compared to the undried sample. In the case of [BMIM][PF<sub>6</sub>], the viscosity data presented by Jacquemin et al.<sup>28</sup> (water in mass fraction  $0.19 \times 10^3$ ) and

**Figure 3.** Temperature dependent relative deviations ( $\delta = (\eta_{\text{fit}} - \eta_{\text{lit}})/\eta_{\text{fit}}$ ) of fluidity for [BMIM][PF<sub>6</sub>] ( $\circ$ ,  $\nabla$ ,  $\square$ ,  $\star$ ,  $\Delta$ ,  $\blacktriangle$  and  $\blacksquare$ ) and [EMIM][MeSO<sub>3</sub>] (right facing triangle) between our fitted data for ( $1/\eta$ ) and those reported in literature.  $\circ$ , Fan et al.;<sup>24</sup>  $\nabla$ , Baker et al.;<sup>25</sup>  $\square$ , Tokuda et al.;<sup>26</sup>  $\star$ , Jiqin et al.;<sup>27</sup>  $\Delta$ , Jacquemin et al.;<sup>28</sup>  $\blacktriangle$ , Seddon et al.;<sup>29</sup>  $\blacksquare$ , Pereiro et al.;<sup>30</sup> right facing triangle, Hass et al.;<sup>33</sup> and  $-$ , present work.

Seddon et al.<sup>29</sup> (76 ppm water containing samples) show good agreement. However, our data is about 9% lower for viscosity, except for the higher values of Pereiro et al.<sup>30</sup> For comparison of viscosity of [EMIM][MeSO<sub>3</sub>], we have only three data points available in literature, in which Himmler et al.<sup>31</sup> and Cooper and O'Sullivan<sup>32</sup> report single value of viscosity of [EMIM][MeSO<sub>3</sub>] at 298 K hence we could not compare our results with their values while Hasse et al.<sup>33</sup> have reported temperature dependent viscosity of [EMIM][MeSO<sub>3</sub>]. Our viscosity data of [EMIM][MeSO<sub>3</sub>] complied well with the work of Hasse et al.<sup>33</sup>

**Density.** Our experimental density values for three ILs obtained over a range of temperature and at atmospheric

**Table 2.** Experimental Densities ( $\rho^a$ ) of the ILs over the Temperature Range (303.0 to 333.0) K and Pressure  $p = 0.1 \text{ MPa}$ <sup>b</sup>

$T^c$ K	$\rho^a/\text{g}\cdot\text{cm}^{-3}$		
	[BMIM][PF <sub>6</sub> ]	[BMIM][OscO <sub>4</sub> ]	[EMIM][MeSO <sub>3</sub> ]
303.0	1.3594	1.0602	1.2470
308.0	1.3582	1.0578	1.2432
313.0	1.3532	1.0532	1.2402
318.0	1.3498	1.0508	1.2376
323.0	1.3468	1.0464	1.2344
328.0	1.3438	1.0422	1.2324
333.0	1.3406	1.0398	1.2302

<sup>a</sup> $u(\rho) = 0.0002 \text{ g}\cdot\text{cm}^{-3}$ . <sup>b</sup>Standard uncertainties. <sup>c</sup> $u(T) = \pm 0.1 \text{ K}$ .

pressure have been summarized in Table 2. The density values for all the ILs can be presented by single eq given as

$$\rho = a - bT \quad (3)$$

In eq 3,  $T$  is the temperature (in K) and  $a$  and  $b$  are the fit parameters as given in Table 3. From Figure 4, it can be seen that measured density of all the ILs decreases with increase in

**Table 3.** Coefficients  $a$  and  $b$  of eq 3 for the Density of [BMIM][PF<sub>6</sub>], [BMIM][OCSO<sub>4</sub>], and [EMIM][MeSO<sub>3</sub>] from the Temperature Range (303.0 to 333.0) K<sup>a</sup>

IL	$a$	$b \cdot 10^{-4}$	$R^2$
[BMIM][PF <sub>6</sub> ]	1.558 ( $\pm$ 0.009)	6.5460 ( $\pm$ 0.2763)	0.9894
[BMIM][OCSO <sub>4</sub> ]	1.274 ( $\pm$ 0.008)	7.0440 ( $\pm$ 0.2524)	0.9924
[EMIM][MeSO <sub>3</sub> ]	1.414 ( $\pm$ 0.008)	5.5360 ( $\pm$ 0.2386)	0.9890

<sup>a</sup>Standard deviations are given as  $\pm$  in parentheses.

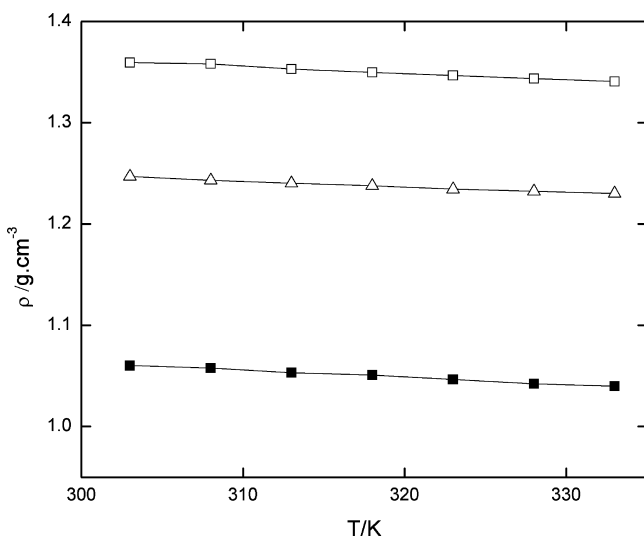


**Figure 4.** Experimental densities of the ILs at different temperature. □, [BMIM][PF<sub>6</sub>], ■, [BMIM][OCSO<sub>4</sub>] and Δ, [EMIM][MeSO<sub>3</sub>], —, linear fit.

temperature. The density of [BMIM][PF<sub>6</sub>] is more than [BMIM][OCSO<sub>4</sub>] and that of [BMIM][OCSO<sub>4</sub>] is larger than [EMIM][MeSO<sub>3</sub>]. Density of ILs having same imidazolium cation is found to increase with increase in molecular weight of the anion.<sup>34</sup> However, density of [BMIM][PF<sub>6</sub>] is larger than [BMIM][OCSO<sub>4</sub>], although molecular weight of anion [OCSO<sub>4</sub>] is larger than anion [PF<sub>6</sub>]. This is possibly due to the long alkyl chain of anion (hence, strongly asymmetric) which favors loose packing of ions and results low density. Similar behavior has been observed by Gardas et al.<sup>35</sup> for imidazolium based cations where increase in the liquid density is not directly proportional to rise in molecular weight of the anions. This can be explained by the stronger localized charge in [PF<sub>6</sub>] anion than on [OCSO<sub>4</sub>], which gives stronger ion pairing of [PF<sub>6</sub>] with [BMIM] cation resulting in higher density.

Relative deviations of the measured densities reported in literature from the fits of our experimental values (according to eq 3) for the IL ([BMIM][PF<sub>6</sub>]) is shown in Figure 5. In the case of [BMIM][PF<sub>6</sub>], density data reported by Yoshimura et al.<sup>36</sup> agree reasonably well with our data. In Figure 5, maximum deviation with respect to Kumar<sup>37</sup> is about 0.4%. Similarly, our results of densities for [BMIM][OCSO<sub>4</sub>] (see the Supporting Information, Figure S1) and [EMIM][MeSO<sub>3</sub>] agree well with the works of Singh et al.<sup>43</sup> and Hasse et al.<sup>33</sup> respectively. However, maximum deviation for [BMIM][OCSO<sub>4</sub>] is about 0.5% with respect to the data reported by Jacquemin et al.<sup>44</sup> whereas about 0.9% for [BMIM][OCSO<sub>4</sub>] relative to data presented by Hasse et al.<sup>33</sup> for [EMIM][MeSO<sub>3</sub>]. At present, only four data points for the density of [EMIM][MeSO<sub>3</sub>] are

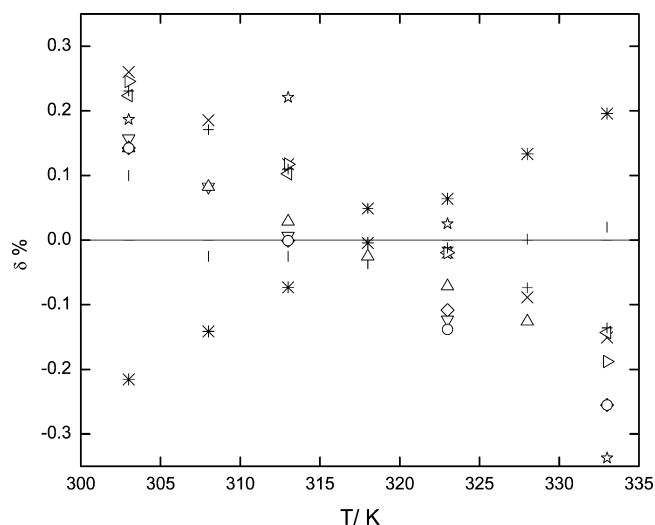


**Figure 5.** Relative deviations ( $\delta = (\rho_{\text{lit}} - \rho_{\text{fit}}) / \rho_{\text{fit}}$ ) between our fitted data for density of [BMIM][PF<sub>6</sub>] and those reported in literature. +, Fan et al.;<sup>24</sup> ○, Jacquemin et al.;<sup>28</sup> ☆, Seddon et al.;<sup>29</sup> \*, Pereiro et al.;<sup>30</sup> l, Yoshimura et al.;<sup>36</sup> ×, Kumar;<sup>37</sup> left facing triangle, Harris et al.;<sup>38</sup> ◇, Jacquemin et al.;<sup>39</sup> Δ, Kabo et al.;<sup>40</sup> right facing triangle, Jacquemin et al.;<sup>41</sup> ▽, Huo et al.;<sup>42</sup> —, present work.

available in the literature. Only Hasse et al.<sup>33</sup> have given temperature variation of density of [EMIM][MeSO<sub>3</sub>] and their data is about 0.8% higher than our values. However, Himmler et al.,<sup>31</sup> Cooper and O'Sullivan,<sup>32</sup> and Arce et al.<sup>45</sup> reported density of [EMIM][MeSO<sub>3</sub>] as 1.2400 g/cm<sup>3</sup> (at temperature of 298.15 K), 1.2400 g/cm<sup>3</sup> (at room temperature), and 1.2437 g/cm<sup>3</sup> (at temperature of 298.15 K), which is consistent with our results. It can be seen that, deviations from the fits of our experimental density data (according to eq 3) and the literature values lie beyond the measurement uncertainty of  $2 \times 10^{-4}$  g/cm<sup>3</sup> in all the cases, which may be attributed to variations in purity, water content, temperature and handling of ILs in previous report.

**Surface Tension.** Surface tension is the most fundamental property in surface science. Therefore, we have studied surface tension of [BMIM][PF<sub>6</sub>], [BMIM][OCSO<sub>4</sub>] and [EMIM][MeSO<sub>3</sub>] over a range of temperature between (303.0 to 333.0) K and the values of surface tension are listed in Table 4. Figure 6 depicts our experimental results of surface tension with temperature. From Figure 6, it can be seen that the surface tension of these ILs decreases linearly with temperature.

**Table 4.** Surface Tensions ( $\gamma^a$ /mN·m<sup>-1</sup>) of the ILs at Atmospheric Pressure  $p = 0.1$  MPa and Temperature from (303.0 to 333.0) K<sup>b</sup>

$T^c$ K	$\gamma$ /mN·m <sup>-1</sup>		
	[BMIM][PF <sub>6</sub> ]	[BMIM][OCSO <sub>4</sub> ]	[EMIM][MeSO <sub>3</sub> ]
303.0	45.3	35.7	47.8
308.0	45.0	35.2	47.4
313.0	44.7	34.9	47.0
318.0	44.4	34.7	46.7
323.0	44.1	34.3	46.1
328.0	43.8	33.9	45.7
333.0	43.5		45.4

<sup>a</sup> $u(\gamma) = 0.1$  mN·m<sup>-1</sup>. <sup>b</sup>Standard uncertainties. <sup>c</sup> $u(T) = \pm 0.1$  K.



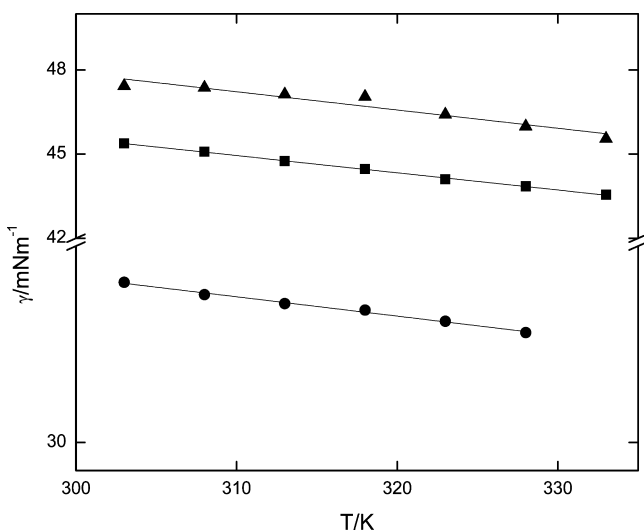


**Figure 6.** Temperature dependent surface tensions of the ILs. ●, [BMIM][OCSO<sub>4</sub>], ■, [BMIM][PF<sub>6</sub>], ▲, [EMIM][MeSO<sub>3</sub>], —, linear fit.

Temperature variation of surface tension can be represented by a single eq as given below

$$\gamma = a - bT \quad (4)$$

where  $\gamma$  is the surface tension and  $a$  and  $b$  are fitting parameters. The value of fit parameters " $a$ " and " $b$ " can be identified as surface enthalpy and surface entropy respectively in Table 5. From Figure 6, it can also be seen that [EMIM][MeSO<sub>3</sub>] has higher surface tension while for [BMIM][OCSO<sub>4</sub>] it is the least in the investigated temperature range and both cations and anions distinctively contribute to the surface tension. Ghatte et al.<sup>46</sup> showed that surface tension of short alkyl chain ILs is mainly governed by the nature of their anions, however, this effect becomes less with increasing alkyl chain length. Similarly, Law and Wastson<sup>47</sup> showed that surface tension is found to decrease with increase in the alkyl chain length of IL cation. They also indicated that for the same cation, surface tension increases with size of the anion. The results found for [BMIM] and [EMIM] cation comply well with former prediction of Law and Wastson.<sup>47</sup> However, in the light of experimental values of [BMIM][OCSO<sub>4</sub>] and [BMIM][PF<sub>6</sub>] which have the same cation, we found that contribution of anion on the surface tension is very significant but our result is opposite to that of Law and Wastson.<sup>47</sup> The IL ([BMIM][OCSO<sub>4</sub>]) with largest anion shows lower surface tension than [BMIM][PF<sub>6</sub>]. However, if we compare surface tension of [EMIM][MeSO<sub>3</sub>] with either [BMIM][PF<sub>6</sub>] or [BMIM][OCSO<sub>4</sub>] it can be seen that [BMIM][OCSO<sub>4</sub>] has the lowest surface tension although it has largest anion whereas [EMIM][MeSO<sub>3</sub>] has the highest value of surface tension but has

smaller alkyl chain of cation as well as smaller anion. Therefore, we can not explain surface tension of ILs only on the basis of the size of the cation and anion. Therefore, for complete explanation of surface tension, we must include electrostatic interaction between cation and anion. These interactions are governed by the Lewis basicity of anion.<sup>48</sup> For the same cation, Lewis basicity is large for the anion having locally large negative charge with an asymmetric distribution and is small for anions having symmetric charge distribution of low negative charge. Highest surface tension observed for [EMIM][MeSO<sub>3</sub>] in this study can be explained on the basis of above discussion. In case of the IL ([EMIM][MeSO<sub>3</sub>]), anion ([MeSO<sub>3</sub>]) has strong negative charge and lowest charge delocalization therefore, Lewis basicity of anion ([MeSO<sub>3</sub>]) is larger and hence electrostatic interaction is larger which results in higher surface tension of [EMIM][MeSO<sub>3</sub>]. For [BMIM][OCSO<sub>4</sub>], surface tension is smaller because large alkyl chain of anion prevents the strong electrochemical interaction between anion and cation. Our result is similar to the finding of Hasse et al.<sup>33</sup> If we compare surface tension of [BMIM][PF<sub>6</sub>] and [BMIM][OCSO<sub>4</sub>], it is found that an increase in the size of anion results decrease in the surface tension. As stated earlier, large size of anion (which results less charge density) prevents the formation of stronger electrochemical interaction between cation and anion. The results found for the same cation of ILs containing [PF<sub>6</sub>] and [OCSO<sub>4</sub>] anions comply well with the findings of Freire et al.<sup>49</sup> Hence, energetic interactions are more relevant for better understanding of surface tension.

As discussed above and observed earlier,<sup>47,49–52</sup> the surface tension of the measured ILs has been found to decrease with increase in temperature. Relative deviations between the fit of our experimental data and values reported in literature are given in Figure 7. From Figure 7, it can be seen that the maximum deviation is about 5% relative to Kilaru et al.'s data. The surface tension reported by Klomfar et al. {(a) Wilhelmy Plate method (b) du Nouy ring method}<sup>53</sup> and Freire et al.<sup>49</sup> are slightly lower than our measured values. On the other hand the surface tension values given by Ghatee et al.<sup>46</sup> and Kilaru et al.<sup>54</sup> are higher than our values with average deviation of 3.5 and 4.2%, respectively. Only one recent data on surface tension for [BMIM][OCSO<sub>4</sub>] reported by Wandschneider et al.<sup>55</sup> is available for comparison at the temperature range (308.0 to 328.0) K. The average deviation between our data (fit data) and the data of surface tension reported by Wandschneider et al.<sup>55</sup> is large. However, no other surface tension data is available in the literature for comparison nonetheless, the surface tension of [EMIM][MeSO<sub>3</sub>] as reported by Hasse et al.<sup>33</sup> is 50.7 mN·m<sup>−1</sup> (at 293.15 K). A comparison is made with the extrapolated value from our experimental data (using eq 4) at 293.15 K, which is 48.6 mN·m<sup>−1</sup> which is slightly lower than the values reported by Hasse et al.<sup>33</sup>

**Table 5.** Surface Thermodynamic Properties of the ILs<sup>a</sup>

IL	surface enthalpy/J·m <sup>−2</sup> ·10 <sup>−2</sup>		surface entropy/J·m <sup>−2</sup> ·K <sup>−1</sup> ·10 <sup>−5</sup>	
	exp.	lit. values	exp.	lit. values
[BMIM][OCSO <sub>4</sub> ]	5.65 (± 0.08)		6.980 (± 0.003)	
[BMIM][PF <sub>6</sub> ]	6.30 (± 0.02)	6.23 (± 0.05) <sup>b</sup> 6.74 (± 0.57) <sup>c</sup>	6.130 (± 0.001)	6.2 (± 0.1) <sup>b</sup> 6.52 (± 0.001) <sup>c</sup>
[EMIM][MeSO <sub>3</sub> ]	7.19 (± 0.50)		8.096 (± 0.010)	

<sup>a</sup>Standard deviations are given as ± in parentheses. <sup>b</sup>Freire et al.<sup>49</sup> <sup>c</sup>Kilaru et al.<sup>54</sup>

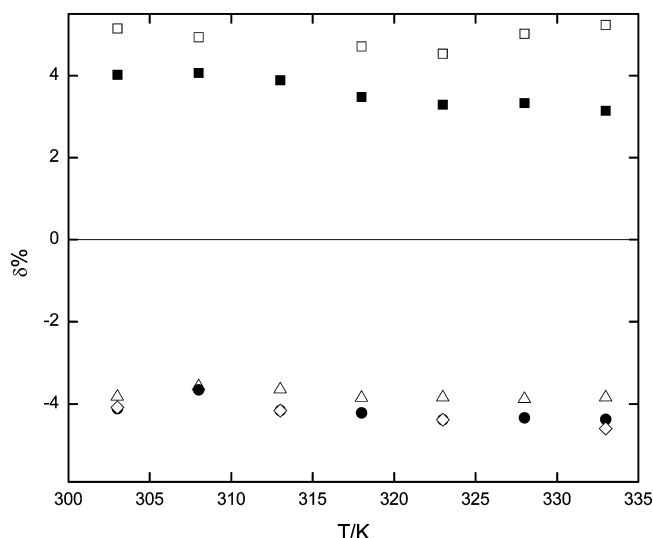


**Figure 7.** Relative deviations ( $\delta = (\gamma_{\text{lit}} - \gamma_{\text{fit}})/\gamma_{\text{fit}}$ ) between our fitted data for surface tension of [BMIM][PF<sub>6</sub>] and those reported in literature. ■, Gate et al.;<sup>46</sup> ◇, Freire et al.;<sup>49</sup> Δ, and ●, Klomfar et al.;<sup>53</sup> □, Kilaru et al.;<sup>54</sup> —, present work.

**Surface Thermodynamic Properties for Pure ILs.** It is possible to derive the surface thermodynamic properties viz. surface entropy, surface enthalpy etc. by measuring temperature dependence of surface tension. The basic thermodynamic relationship applied to the surface of a homogeneous liquid is

$$H^{\gamma} = G^{\gamma} + TS^{\gamma} \quad (5)$$

where  $H^{\gamma}$  is surface enthalpy,  $G^{\gamma}$  is the Gibbs energy as related to the surface tension of homogeneous liquid,  $T$  is temperature (in K), and  $S^{\gamma}$  surface entropy. Surface entropy per unit area is given by the change in the surface tension with temperature as

$$S^{\gamma} = -\frac{d\gamma}{dT} \quad (6)$$

while the surface enthalpy,  $H^{\gamma}$ , can be defined as

$$H^{\gamma} = \gamma - T\left(\frac{d\gamma}{dT}\right) \quad (7)$$

The values of surface entropy and surface enthalpy can easily be obtained by linear surface tension–temperature profiles. In a linear surface tension–temperature profile, the intercept can be identified as surface enthalpy (coefficient “ $a$ ” in eq 3) and the slope gives surface entropy (coefficient “ $b$ ” in eq 3), which is assumed to be temperature independent. The values of these surface thermodynamic properties of the ILs have been evaluated and listed in Table 5 and compared with available values from other authors, whenever available. If we compare surface entropy of the studied IL with the values for organic solvents viz. benzene ( $S^{\gamma} = 13 \cdot 10^{-5} \text{ J} \cdot \text{m}^{-2} \cdot \text{K}^{-1}$  at (20–80) °C),<sup>56</sup> it is found that surface entropy of the ILs is remarkably low. The lower values of surface entropy of studied ILs suggest an enhancement of surface organization as well as highly structured liquid phase which is in agreement with the results reported for other ILs.<sup>57</sup> In a recent study, Freire et al.<sup>49</sup> shows that (i) surface entropy increases with the size of alkyl chain of IL cation (ii) they have also suggested that surface entropy is largely affected by anion compared to alkyl chain of cation. Our results do not agree with the first finding of Freire et al.,<sup>49</sup> as it can be seen from Table 5 that the surface entropy of

[EMIM][MeSO<sub>3</sub>] is larger than [BMIM][PF<sub>6</sub>] and [BMIM][OCSO<sub>4</sub>]. Therefore, it is concluded that in the present case surface entropy is more affected by the type of anion which is in good agreement with second conclusion by Freire et al.<sup>49</sup> Surface enthalpy of [EMIM][MeSO<sub>3</sub>] is larger than that of [BMIM]PF<sub>6</sub> and [BMIM][OCSO<sub>4</sub>]. If we compare surface energy of [EMIM] and [BMIM] cation of the ILs, it is found that on increasing the alkyl chain length of the cation of the ILs, surface energy decreased which is consistent with available values.<sup>49,58</sup> Reduction in the surface enthalpy with increase in alkyl chain length of cation of the ILs is possibly due to reduction on hydrogen bond strength between cation and anion due to dispersion of the charge on a relatively large size cation. Importantly, we have observed that surface enthalpy not only depends on alkyl chain length but also depends on type of anion. Surface enthalpy of the IL with [PF<sub>6</sub>] anion is larger than [OCSO<sub>4</sub>] anion.

**Critical Temperature.** Like many other thermophysical properties (viz. viscosity, density, surface tension, etc.), critical temperature is also one of the most relevant thermophysical properties because it can be used to develop the thermodynamic model for fluids and in many corresponding states, correlation for the equilibrium. However, limited data is available in literature for critical temperature of ILs, possibly because of difficulties in determining critical temperature experimentally since, many ILs decompose as the temperature approaches the normal boiling point. Therefore, in order to enhance the knowledge about this important thermophysical property, we have estimated critical temperature using Guggenheim<sup>59</sup> and Eotvos<sup>60</sup> empirical equations using temperature dependence of surface tension as given below.

$$\gamma = k \left(1 - \frac{T}{T_c}\right)^{\phi} \quad (8)$$

$$\gamma \left(\frac{M}{\rho}\right)^{2/3} = k(T_c - T) \quad (9)$$

where  $\gamma$  is the surface tension.  $T_c$  is the critical temperature,  $\phi$  is an exponent whose value is 1.22,  $M$  is the molecular weight,  $\rho$  is the density of the IL, and  $k$  is the total surface energy of the liquid, which equals the surface enthalpy as long as there is negligible volume change due to thermal expansion at temperature far away from the critical temperature ( $T_c$ ). Use of Guggenheim equation reflects the fact that  $\gamma$  becomes null when the temperature of the liquid reaches the critical point<sup>61</sup> and is based on corresponding states correlation.<sup>62</sup> This assumption follows from the view that, at critical point there exists no clear distinction between the liquid and vapor phase. The values of critical temperature estimated in the present study are compared with available literature values (Table 6).

**Ultrasonic Velocity.** Ultrasonic velocity<sup>64</sup> is one of the important parameters in ultrasonic spectroscopy. Ultrasonic waves interact with the materials and generate accurate information about molecular phenomenon and hence can be used as characterizing tool in many fields of science and technology. Table 7 shows our experimental results of ultrasonic velocity for [BMIM][PF<sub>6</sub>], [BMIM][OCSO<sub>4</sub>], and [EMIM][MeSO<sub>3</sub>] at 4 MHz. From Figure 8, it can be seen that ultrasonic velocity of these three imidazolium based ILs is found to decrease with increase in temperature, which shows good agreement with available literature<sup>30,37,43,65</sup> values. Ultrasonic velocity measurement along with density offers a

**Table 6.** Predicted Critical Point Temperatures ( $T_c$ ) and Parameters from Guggenheim and Eotvos Equations for the ILs<sup>a</sup>

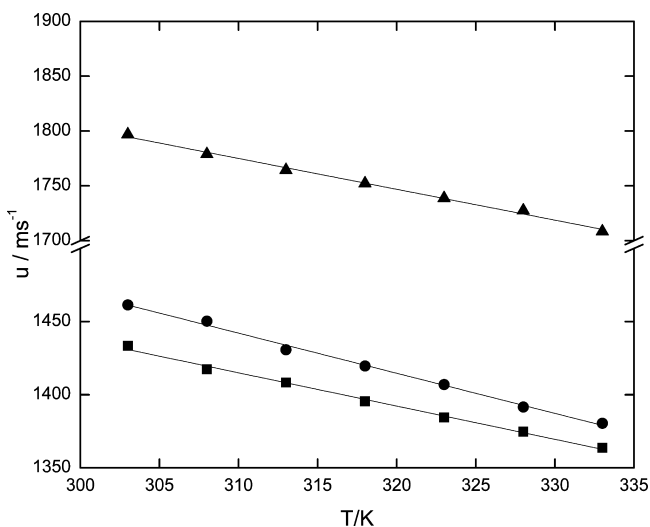
IL	Guggenheim parameters		Eotvos parameter	
	A	$T_c$	K	$T_c$
[BMIM][OscSO <sub>4</sub> ]	56.5 (± 0.9)	821 (± 20)	2.557 (± 0.004)	967 (± 1)
[BMIM][PF <sub>6</sub> ]	64.0 (± 0.3)	1042 (± 11)	1.664 (± 0.002)	1263 (± 2)
		1102 <sup>b</sup>		1187 <sup>b</sup>
		958 (± 17) <sup>c</sup>		977 (± 22) <sup>c</sup>
[EMIM][MeSO <sub>3</sub> ]	72 (± 5)	903 (± 105)	1.989 (± 0.002)	1027 (± 1)

<sup>a</sup>Standard deviations are given as ± in parentheses. <sup>b</sup>Rebello et al.;<sup>63</sup> with relative deviation of 13.1% (Guggenheim) and 17.7% (Eotvos). <sup>c</sup>Freire et al.<sup>49</sup>

**Table 7.** Temperature Dependent Ultrasound Velocity ( $u^a$ /ms<sup>-1</sup>) of the ILs at a Frequency 4 MHz and at Constant Pressure  $p = 0.1$  MPa<sup>b</sup>

$T^c$	$u$ /ms <sup>-1</sup>		
K	[BMIM][PF <sub>6</sub> ]	[BMIM][OscSO <sub>4</sub> ]	[EMIM][MeSO <sub>3</sub> ]
303.0	1433.2	1461.2	1796.3
308.0	1416.8	1450.4	1777.8
313.0	1407.9	1429.7	1763.9
318.0	1395.4	1419.3	1752.3
323.0	1383.6	1406.4	1738.1
328.0	1374.3	1390.7	1727.0
333.0	1362.9	1380.3	1708.0

<sup>a</sup> $u(u) = \pm 0.03$  ms<sup>-1</sup>. <sup>b</sup>Standard uncertainties. <sup>c</sup> $u(T) = \pm 0.1$  K.

**Figure 8.** Temperature dependent ultrasonic velocity ( $u$ ) of the ILs. ●, [BMIM][OscSO<sub>4</sub>], ■, [BMIM][PF<sub>6</sub>], ▲, [EMIM][MeSO<sub>3</sub>], —, linear fit.

feasible method to determine the isentropic compressibility,  $k_s$ . Isentropic compressibility<sup>66</sup>  $k_s$  of liquids is defined by

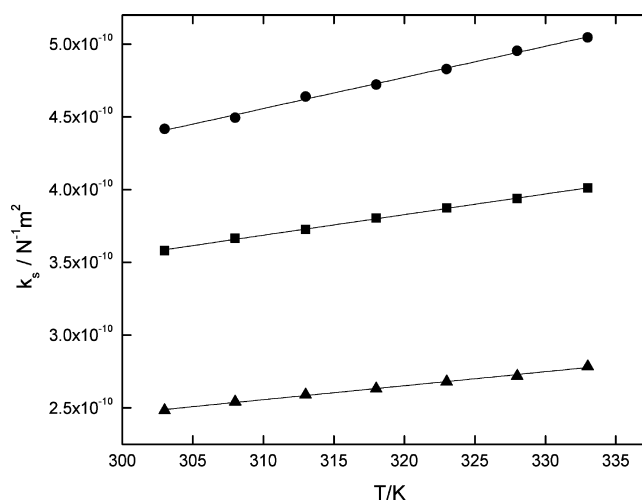
$$k_s = -\frac{1}{V} \left( \frac{\partial V}{\partial P} \right)_s \quad (10)$$

where  $V$  is the total liquid volume. Isentropic compressibility is significant thermodynamic parameter and depends on the

structure of liquid, since, a change in volume due to application of pressure will be different for liquids having different structure. The isentropic compressibility,  $k_s$  of a liquid medium is determined from the density  $\rho$  of liquid and ultrasonic velocity,  $u$  (the phase velocity of longitudinal wave within the medium) by Newton–Laplace eq

$$k_s = \frac{1}{\rho u^2} \quad (11)$$

Temperature dependent isentropic compressibility of the ILs at 4 MHz is shown in Figure 9. From Figure 9, it can be seen that

**Figure 9.** Temperature dependent isentropic compressibility ( $k_s$ ) of the ILs. ■, [BMIM][PF<sub>6</sub>], ●, [BMIM][OscSO<sub>4</sub>], ▲, [EMIM][MeSO<sub>3</sub>], —, linear fit.

the isentropic compressibility for the studied ILs is found to increase with rise in temperature. The compressibility of ILs studied in the present case is less than the organic liquids due to strong columbic interactions between cations and anions of ILs. From the isentropic compressibility of [BMIM][PF<sub>6</sub>] and [BMIM][OscSO<sub>4</sub>], it is found that the ILs which have greater molecular volume are more compressible. Also, it is evident that isentropic compressibility of the ILs with common cation increases with anion size. However, values of isentropic compressibility for [BMIM][PF<sub>6</sub>] and [EMIM][MeSO<sub>3</sub>] suggest that it also increases with increase in alkyl chain length of cation. This is possibly due to large free volume available either if we increase size of cation or anion. For the same cation of ILs, isentropic compressibility follows the following order for different anions  $[PF_6] < [OscSO_4]$ .

From Figure 10, it can be seen that there is a negative deviation of 0.03 to 0.6 respectively for the data given by Pereiro et al.<sup>30</sup> and Kumar<sup>37</sup> et al. with respect to our data for [BMIM][PF<sub>6</sub>] while for [BMIM][OscSO<sub>4</sub>], the average relative deviation in the experimental velocity with the data reported by Singh et al.<sup>43</sup> and Davila et al.<sup>65</sup> relative to our data is within ± 0.4 %. Results of ultrasonic velocity for [EMIM][MeSO<sub>3</sub>] could not be compared due to unavailability of literature data. A comparison has been made for isentropic compressibility evaluated using density and velocity data reported by Pereiro et al.<sup>30</sup> and Kumar<sup>37</sup> for [BMIM][PF<sub>6</sub>] and Singh et al.<sup>43</sup> and Davila et al.<sup>65</sup> for [BMIM][OscSO<sub>4</sub>] to that of our work (see Figure 11). Our isentropic compressibility data comply well with the work of Pereiro et al.<sup>30</sup> for [BMIM][PF<sub>6</sub>] (with an



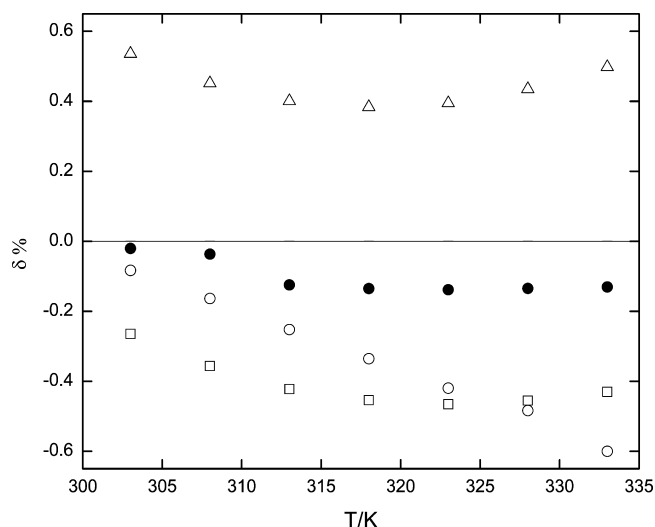


**Figure 10.** Relative deviations ( $\delta = (u_{lit} - u_{fit})/u_{fit}$ ) between our fitted data for ultrasonic velocities of [BMIM][PF<sub>6</sub>] and [BMIM][OcsO<sub>4</sub>] to those reported in literature. ●, Pereiro et al.;<sup>30</sup> ○, Kumar;<sup>37</sup> △, Singh et al.;<sup>43</sup> □, Davila et al.;<sup>65</sup> —, present work.

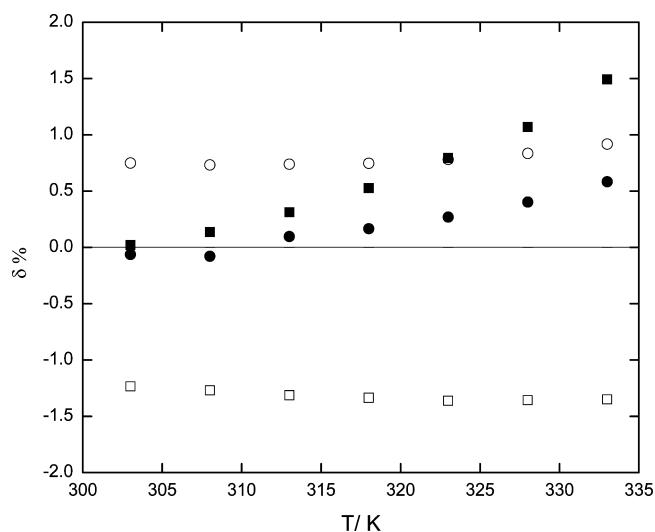


**Figure 11.** Relative deviations ( $\delta = (k_{s,fit} - k_{s,lit})/k_{s,lit}$ ) between our fitted data for isentropic compressibility of [BMIM][PF<sub>6</sub>] and [BMIM][OcsO<sub>4</sub>] to those reported in literature. ■, Pereire et al.;<sup>30</sup> ●, Kumar;<sup>37</sup> ○, Singh et al.;<sup>43</sup> ○, Davila et al.;<sup>65</sup> —, present work. Fill symbol for [BMIM][PF<sub>6</sub>] and empty symbol for [BMIM][OcsO<sub>4</sub>].

average relative deviation between  $-0.07$  to  $0.3\%$ ). However, isentropic compressibility reported by Singh et al.<sup>43</sup> is slightly higher than our values. For [BMIM][OcsO<sub>4</sub>], isentropic compressibility reported by Davila et al.<sup>65</sup> is slightly higher (with an average relative deviation of  $0.7\%$ ) than our present data while it is lower as compared to work of Singh et al.<sup>43</sup> Due to unavailability of isentropic compressibility data for [EMIM][MeSO<sub>3</sub>] in literature, we could not compare our data.

**Molecular Volume.** The molecular volume ( $V_{mol}$ ) of the [BMIM][PF<sub>6</sub>], [BMIM][OcsO<sub>4</sub>], and [EMIM][MeSO<sub>3</sub>] can be evaluated from the knowledge of density using eq

$$V_{mol} = M/N_{\rho} \quad (12)$$

where  $M$  is the molar mass (284.18, 348.50, and 206.26 for [BMIM][PF<sub>6</sub>], [BMIM][OcsO<sub>4</sub>], and [EMIM][MeSO<sub>3</sub>],

respectively),  $N$  is Avogadro's number, and  $\rho$  the is density (we used fitted values of experimental densities for evaluating  $V_{mol}$  and molar volume). Table 8 shows molar and molecular

**Table 8.** Molar and Molecular Volume of the ILs at  $T^a = (303.0 \text{ and } 333.0) \text{ K}^b$

IL	molar volume/ cm <sup>3</sup> .mol <sup>-1</sup>		molecular volume/nm <sup>3</sup>	
	T/K			
	303.0	333.0	303.0	333.0
[BMIM][PF <sub>6</sub> ]	208.95	212.01	0.3469	0.3519
[BMIM][OCSO <sub>4</sub> ]	328.56	335.24	0.5455	0.5566
[EMIM][MeSO <sub>3</sub> ]	165.51	167.75	0.2747	0.2785

<sup>a</sup> $u(T) = \pm 0.1 \text{ K}$ . <sup>b</sup>Standard uncertainties.

volume of the ILs at (303.0 and 333.0) K. From Table 8, it is evident that an increase in the molecular volumes of the ILs with temperature has been observed.

**Thermal Expansion Coefficient.** Thermal expansion coefficient also known as isobaric expansivity ( $\alpha_p$ ) is an important thermodynamic parameter which reflects changes in the liquid volume. The evaluation of the volumetric properties with temperature can be expressed by evaluating thermal expansion coefficient, which is generally based on temperature dependence of density. Thermal expansion coefficient is defined as

$$\alpha_p \equiv \frac{1}{V} \left( \frac{\partial V}{\partial T} \right)_p \equiv -\frac{1}{\rho} \left( \frac{\partial \rho}{\partial T} \right)_p \quad (13)$$

where  $V$  stands for molar volume,  $T$  for temperature, and  $P$  for the pressure. Using eq 13, we have calculated  $\alpha_p$  of the three ILs by monitoring fractional change in volume with rise in temperature e.g. if temperature was raised from (20 to 25) °C  $\alpha_p$  was determined at 20 °C by observing  $dV$  for this 5 °C change in temperature (in our pycnometer a sensitive capillary tube having equispaced graduated scales was fitted whose one division was equal to 0.001 cc so, the volume change was measured very accurately) and using  $V$  value. Similarly,  $\alpha_p$  was measured at different temperatures. As discussed above, temperature dependence of density and molar volume of the ILs are linear therefore can be easily obtained by linear fit of density. From Figure 12 it can be seen that a very small variation of thermal expansion coefficient has been observed with rise in temperature. Therefore, we conclude that thermal expansion coefficients of the ILs have less thermal expansivity which is consistence with the available literature<sup>35,67</sup> data. The values of thermal expansion coefficients of the ILs vary between  $(4.5 \cdot 10^{-4} \text{ to } 6.7 \cdot 10^{-4}) \text{ K}^{-1}$ . Gu and Brennecke<sup>67</sup> have found a small change in the value of thermal expansion coefficient for many ILs with temperature. Gardas et al.<sup>35</sup> have found that even in the wide range of temperature many ILs appear to not expand distinctly.

## CONCLUSION

In summary, we have reported new experimental data on several thermophysical properties namely, viscosity, density, surface tension, ultrasonic velocity etc over a wide range of temperature. Using these data we have also derived thermal expansion coefficient, surface enthalpy, surface entropy, critical temperature (using Eotvos and Guggenheim correlations) and isentropic compressibility of three imidazolium based ILs viz. [BMIM][OcsO<sub>4</sub>], [BMIM][PF<sub>6</sub>], and [EMIM][MeSO<sub>3</sub>] and

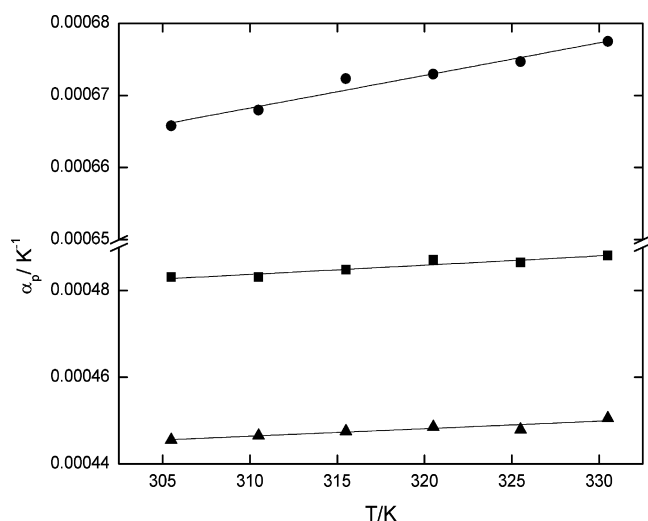


**Figure 12.** Temperature dependent thermal expansion coefficient of the ILs. ■, [BMIM][PF<sub>6</sub>], ●, [BMIM][OCSO<sub>4</sub>], ▲, [EMIM][MeSO<sub>3</sub>], —, linear fit.

discussed their dependence on temperature at atmospheric pressure. It is found that temperature dependent fluidity (and hence viscosity) for [BMIM][PF<sub>6</sub>] and [EMIM][MeSO<sub>3</sub>] are different which is explained in terms of relative lengths of the cation chains and the symmetry of charge distribution of anions. Highest value of surface tension is observed for [EMIM][MeSO<sub>3</sub>] and for the same IL cation order of surface tension is [BMIM][PF<sub>6</sub>] > [BMIM][OCSO<sub>4</sub>]. It is found that energetic interactions are more relevant for better understanding of surface tension and surface entropy which largely depend on anion compared to alkyl chain of cation while surface enthalpy of same cationic IL with [PF<sub>6</sub>] anion is larger than [OCSO<sub>4</sub>] anion. Ultrasonic velocity of all three ILs is found to decrease with increase in temperature and isentropic compressibility as well as thermal expansion coefficient of the ILs with common cation increase with anion size, i.e., [PF<sub>6</sub>] < [OCSO<sub>4</sub>]. Also, we conclude that thermal expansion coefficients of the ILs have less expansivity with temperature.

## ■ ASSOCIATED CONTENT

### Supporting Information

Additional figure depicting relative deviations. This material is available free of charge via the Internet at <http://pubs.acs.org>.

## ■ AUTHOR INFORMATION

### Corresponding Author

\*E-mail: [rk Singh\\_17@rediffmail.com](mailto:rk Singh_17@rediffmail.com). Ph: (+91) 542 2307308. Fax: (+91) 542 2368390.

### Funding

R.K.S. is grateful to the UGC, New Delhi, India for providing financial assistance. M.P.S. is thankful to CSIR, New Delhi, India for the award of Senior Research Fellowship (SRF).

### Notes

The authors declare no competing financial interest.

## ■ REFERENCES

(1) Wasserscheid, P.; Welton, T., Eds.; *Ionic Liquids in Synthesis*; WILEY VCH Verlag GmbH & Co. KGaA: Weinheim, Germany, 2007; Vol. 1.

(2) Rogers, R. D.; Seddon, K. R., Eds.; *Ionic Liquids as Green Solvents: Progress and Prospects*; ACS Symposium Series, 856 American Chemical Society: Washington, DC, 2003.

(3) Rogers, R. D.; Seddon, K. R., Eds.; *Ionic Liquids IIIA: Fundamentals, Progress, Challenges, and Opportunities- Properties and Structure*; ACS Symposium Series; Oxford University Press: New York, 2005; Vol. 901.

(4) Hallett, J. P.; Welton, T. Room-Temperature Ionic Liquids: Solvents for Synthesis and Catalysis. 2. *Chem. Rev.* **2011**, *111*, 3508–3576.

(5) Greaves, T. L.; Drummond, C. J. Protic Ionic Liquids: Properties and Applications. *Chem. Rev.* **2008**, *108*, 206–237.

(6) Dupont, J.; Suarez, P. A. Z. Physico-Chemical Processes in Imidazolium Ionic Liquids. *Phys. Chem. Chem. Phys.* **2006**, *8*, 2441–2452.

(7) Armand, M.; Endres, F.; MacFarlane, D. R.; Ohno, H.; Scrosati, B. Ionic-Liquid Materials for the Electrochemical Challenges of the Future. *Nat. Mater.* **2009**, *8*, 621–629.

(8) Nago, H. L.; Lecompte, K.; Hargens, L.; McEwan, A. B. Thermal Properties of Imidazolium Ionic Liquids. *Thermochim. Acta* **2000**, *357–358*, 97–102.

(9) Somers, A. E.; Howlett, P. C.; MacFarlane, D. R.; Forsyth, M. A Review of Ionic Liquid Lubricants. *Lubricants* **2013**, *1*, 3–21.

(10) Chaurasia, S. K.; Singh, R. K.; Chandra, S. Structural and Transport Studies on Polymeric Membranes of PEO Containing Ionic Liquid, EMIM-TY: Evidence of Complexation. *Solid State Ionics* **2011**, *183*, 32–39.

(11) Henderson, W. A.; Passerini, S. Phase Behavior of Ionic Liquid–LiX Mixtures: Pyrrolidinium Cations and TFSI<sup>−</sup> Anions. *Chem. Mater.* **2004**, *16*, 2881–2885.

(12) Fericola, A.; Croce, F.; Scrosati, B.; Watanabe, T.; Ohno, H. LiTFSI-BEPyTFSI as an Improved Ionic Liquid Electrolyte for Rechargeable Lithium Batteries. *J. Power Sources* **2007**, *174*, 342–348.

(13) Ke, C.; Li, J.; Li, X.; Shao, Z.; Yi, B. Protic ionic liquids: an alternative proton-conducting electrolyte for high temperature proton exchange membrane fuel cells. *RSC Adv.* **2012**, *2*, 8953–8956.

(14) Chandra, S. Recent Trends in High Efficiency Photo-Electrochemical Solar Cell Using Dye-Sensitised Photo-Electrodes and Ionic Liquid Based Redox Electrolytes. *Proc. Natl. Acad. Sci. Sect. A Phys. Sci.* **2012**, *82* (1), 5–19.

(15) Shaikh, J. S.; Pawar, R. C.; Devan, R. S.; Ma, Y. R.; Salvi, P. P.; Kolekar, S. S.; Patil, P. S. Synthesis and characterization of Ru doped CuO thin films for supercapacitor based on Bronsted acidic ionic liquid. *Electrochim. Acta* **2011**, *56*, 2127–2134.

(16) Serrano-Santos, M. B.; Llobet, E.; Schäfer, T. Quartz Crystal Microbalance with Dissipation Measurement for Proving the Potential of Ionic Liquids as Selective Sensing Materials. *Procedia Eng.* **2011**, *25*, 1169–1172.

(17) Döbelin, M.; Marcilla, R.; Pozo-Gonzal, C.; Mecerreyes, D. Innovative Materials and Applications Based on Poly(3, 4-ethylenedioxythiophene) and Ionic Liquids. *J. Mater. Chem.* **2010**, *20*, 7613–7622.

(18) Steichen, M.; Dale, P. Synthesis of Trigonal Selenium Nanorods by Electrodeposition from an Ionic Liquid at High Temperature. *Electrochem. Commun.* **2011**, *13*, 865–868.

(19) Singh, M. P.; Singh, R. K.; Chandra, S. Thermal Stability of Ionic Liquid in Confined Geometry. *J. Phys. D: Appl. Phys.* **2010**, *43*, 092001.

(20) Gupta, A. K.; Singh, M. P.; Singh, R. K.; Chandra, S. Low Density Ionogels Obtained by Rapid Gellification of Tetraethyl Orthosilane Assisted by Ionic Liquids. *Dalton Trans.* **2012**, *41*, 6263–6271.

(21) Verma, Y. L.; Singh, M. P.; Singh, R. K. Effect of Ultrasonic Irradiation on Preparation and Properties of Ionogels. *J. Nanomaterials* **2012**, *2012*, 6.

(22) Singh, M. P.; Singh, R. K. Correlation between Ultrasonic Velocity, Surface Tension, Density and Viscosity of Ionic Liquids. *Fluid Phase Equilib.* **2011**, *304*, 1–6.

- (23) Arashiro, E. Y.; Demarquette, N. R. Use of the Pendant Drop Method to Measure Interfacial Tension between Molten Polymers. *Mater. Res.* **1999**, *2*, 23–32.
- (24) Ghatee, M. H.; Zare, M.; Zolghadr, A. R.; Moosavi, F. Temperature Dependence of Viscosity and Relation with the Surface Tension of Ionic Liquids. *Fluid Phase Equilib.* **2010**, *291*, 188–194.
- (25) Noda, A.; Hayamizu, K.; Watanabe, M. Pulsed-Gradient Spin-Echo 1H and 19F NMR Ionic Diffusion Coefficient, Viscosity, and Ionic Conductivity of Non-Chloroaluminate Room-Temperature Ionic Liquids. *J. Phys. Chem. B* **2001**, *105*, 4603–4610.
- (26) Okoturo, O. O.; Vender Noot, T. J. Temperature Dependence of Viscosity for Room Temperature Ionic Liquids. *J. Electroanal. Chem.* **2007**, *568*, 167–181.
- (27) Jiqin, Z.; Jian, C.; Chengyue, Li; Weiyang, F. Viscosities and Interfacial Properties of 1-Methyl-3-butylimidazolium Hexafluorophosphate and 1-Isobutenyl-3-methylimidazolium Tetrafluoroborate Ionic Liquids. *J. Chem. Eng. Data* **2007**, *52*, 812–816.
- (28) Jacquemin, J.; Husson, P.; Padua, A. A. H.; Majer, V. Density and Viscosity of Several Pure and Water-Saturated Ionic Liquids. *Green Chem.* **2006**, *8*, 172–180.
- (29) Seddon, K. R.; Stark, A.; Torres, M.-J. Viscosity and Density of 1-alkyl-3-methylimidazolium Ionic Liquids. In *Clean Solvents: Alternative Media for Chemical Reactions and Processing*; Abraham, M., Moens, L., Eds.; ACS Symposium Series; American Chemical Society: Washington, DC, 2002; Vol. 819, pp 34–49.
- (30) Pereiro, A. B.; Legido, J. L.; Rodriguez, A. Physical Properties of Ionic Liquids Based on 1-alkyl-3-methylimidazolium Cation and Hexafluorophosphate as Anion and Temperature Dependence. *J. Chem. Thermodyn.* **2007**, *39*, 1168–1175.
- (31) Himmler, S.; König, A.; Wasserscheid, P. Synthesis of [EMIM] OH via Bipolar Membrane Electrodialysis—Precursor Production for the Combinatorial Synthesis of [EMIM]-Based Ionic Liquids. *Green Chem.* **2007**, *9*, 935–942.
- (32) Cooper, E. I.; Sullivan, E. J. M. *Proceedings of the 8th International Symposium on Molten Salts*; The Electrochemical Society: Pennington, NJ, 1992; Vols. 92–16, pp 386–396.
- (33) Hasse, B.; Lehmann, J.; Assenbaum, D.; Wasserscheid, P.; Leipertz, A.; Froba, A. P. Viscosity, Interfacial Tension, Density, and Refractive Index of Ionic Liquids [EMIM][MeSO<sub>3</sub>], [EMIM][MeOHPO<sub>2</sub>], [EMIM][OCSO<sub>4</sub>], and [BBIM][NTf<sub>2</sub>] in Dependence on Temperature at Atmospheric Pressure. *J. Chem. Eng. Data* **2009**, *54*, 2576–2583.
- (34) Fredlake, C. P.; Crosthwaite, J. M.; Hert, D. G.; Sudhir, N. V. K. A.; Brennecke, J. F. Thermophysical Properties of Imidazolium-Based Ionic Liquids. *F. J. Chem. Eng. Data* **2004**, *49*, 954–964.
- (35) Gardas, R. L.; Freire, M. G.; Carvalho, P. J.; Marrucho, I. M.; Fonseca, I. M. A.; Ferreira, A. G. M.; Coutinho, J. A. P. High-Pressure Densities and Derived Thermodynamic Properties of Imidazolium-Based Ionic Liquids. *J. Chem. Eng. Data* **2007**, *52*, 80–88.
- (36) Yoshimura, M.; Boned, C.; Baylaucq, A.; Galliéro, G.; Ushiki, H. Influence of the Chain Length on the Dynamic Viscosity at High Pressure of Some Amines: Measurements and Comparative Study of Some Models. *J. Chem. Thermodynamics* **2009**, *41*, 291–300.
- (37) Kumar, A. Estimates of Internal Pressure and Molar Refraction of Imidazolium Based Ionic Liquids as a Function of Temperature. *J. Solution Chem.* **2008**, *37*, 203–214.
- (38) Harris, K. R.; Woolf, L. A. Temperature and Pressure Dependence of the Viscosity of the Ionic Liquid 1-Butyl-3-methylimidazolium Hexafluorophosphate. *J. Chem. Eng. Data* **2005**, *50*, 1777–1782.
- (39) Jacquemin, J.; Husson, P.; Mayer, V.; Cibulka, I. High-Pressure Volumetric Properties of Imidazolium-Based Ionic Liquids: Effect of the Anion. *J. Chem. Eng. Data* **2007**, *52*, 2204–2211.
- (40) Kabo, G. J.; Blokhin, A. V.; Paulechka, Y. U.; Kabo, A. G.; Shymanovich, M. P. Thermodynamic Properties of 1-Butyl-3-methylimidazolium Hexafluorophosphate in the Condensed State. *J. Chem. Eng. Data* **2004**, *49*, 453–461.
- (41) Jacquemin, J.; Husson, P.; Majer, V.; Costa Gomes, M. F. Low-Pressure Solubilities and Thermodynamics of Solvation of Eight Gases in 1-Butyl-3-methylimidazolium Hexafluorophosphate. *Fluid Phase Equilib.* **2006**, *240*, 87–95.
- (42) Huo, Y.; Xia, S.; Ma, P. Solubility of Alcohols and Aromatic Compounds in Imidazolium-Based Ionic Liquids. *J. Chem. Eng. Data* **2008**, *53*, 2535–2539.
- (43) Singh, T.; Kumar, A. Temperature Dependence of Physical Properties of Imidazolium Based Ionic Liquids: Internal Pressure and Molar Refraction. *J. Solution Chem.* **2009**, *38*, 1043–1053.
- (44) Jacquemin, J.; Husson, P.; Majer, V.; Padua, A. H.; Gomes, M. F. C. Thermo physical Properties, Low Pressure Solubilities and Thermodynamics of Solvation of Carbon Dioxide and Hydrogen in Two Ionic Liquids Based on the Alkylsulfate Anion. *Green Chem.* **2008**, *10*, 944–950.
- (45) Arce, A.; Rodriguez, H.; Soto, A. Effect of Anion Fluorination in 1-Ethyl-3-methylimidazolium as Solvent for the Liquid Extraction of Ethanol from Ethyl tert-butyl Ether. *Fluid Phase Equilib.* **2006**, *242*, 164–168.
- (46) Ghatee, M. H.; Zolghadr, A. R. Surface Tension Measurements of Imidazolium-Based Ionic Liquids at Liquid–Vapor Equilibrium. *Fluid Phase Equilib.* **2008**, *263*, 168–175.
- (47) Law, G.; Watson, P. R. Surface Tension Measurements of N-Alkylimidazolium Ionic Liquids. *Langmuir* **2001**, *17*, 6138–6141.
- (48) Tokuda, H.; Tsuzuki, S.; Susan, M. D. A. B. H.; Hayamizu, K.; Watanabe, M. How Ionic are Room-Temperature Ionic Liquids? An Indicator of the Physicochemical Properties. *J. Phys. Chem. B* **2006**, *110*, 19593–19600.
- (49) Freire, M. G.; Carvalho, P. J.; Fernandes, A. M.; Marrucho, I. M.; Queimada, A. J.; Coutinho, J. A. P. Surface Tensions of Imidazolium Based Ionic Liquids: Anion, Cation, Temperature and Water Effect. *J. Colloid Interface Sci.* **2007**, *314*, 621–630.
- (50) Law, G.; Watson, P. R. Surface Orientation in Ionic Liquids. *Chem. Phys. Lett.* **2001**, *345*, 1–4.
- (51) Kim, K.-S.; Demberelnyamba, D.; Shin, B. K.; Yeon, S. H.; Choi, S.; Cha, J. H.; Lee, H.; Lee, C. S.; Shim, J. L. Surface Tension and Viscosity of 1-Butyl-3-methylimidazolium Iodide and 1-Butyl-3-methylimidazolium Tetrafluoroborate, and Solubility of Lithium Bromide + 1-Butyl-3-methylimidazolium Bromide in Water. *Korean J. Chem. Eng.* **2006**, *23*, 113–116.
- (52) Galan Sanchez, L. M.; Meindersma, G. W.; de Haan, A. B. Solvent Properties of Functionalized Ionic Liquids for CO<sub>2</sub> Absorption. *Chem. Eng. Res. Des.* **2007**, *85*, 31–39.
- (53) Klomfar, J.; Souckova, M.; Patek, J. Surface Tension Measurements for Four 1-Alkyl-3-methylimidazolium-Based Ionic Liquids with Hexafluorophosphate Anion. *J. Chem. Eng. Data* **2009**, *54*, 1389–1394.
- (54) Kilaru, P.; Baker, G. A.; Scovazzo, P. Density and Surface Tension Measurements of Imidazolium-, Quaternary Phosphonium-, and Ammonium-Based Room-Temperature Ionic Liquids: Data and Correlations. *J. Chem. Eng. Data* **2007**, *52*, 2306–2314.
- (55) Wandschneider, A.; Lehmann, J. K.; Heintz, A. Surface Tension and Density of Pure Ionic Liquids and Some Binary Mixtures with 1-Propanol and 1-Butanol. *J. Chem. Eng. Data* **2008**, *53*, 596–599.
- (56) Korosi, G.; Kovats, E. S. Density and Surface Tension of 83 Organic Liquids. *J. Chem. Eng. Data* **1981**, *26*, 323–332.
- (57) Santos, L. M. N. B. F.; Canongia Lopes, J. N.; Coutinho, J. A. P.; Esperança, J. M. S. S.; Gomes, L. R.; Marrucho, I. M.; Rebelo, L. P. N. Ionic Liquids: First Direct Determination of their Cohesive Energy. *J. Am. Chem. Soc.* **2007**, *129*, 284–285.
- (58) Restolho, J.; Mata, J. L.; Saramago, B. On the Interfacial Behavior of Ionic Liquids: Surface Tensions and Contact Angles. *J. Colloid Interface Sci.* **2009**, *340*, 82–86.
- (59) Guggenheim, E. A. The Principle of Corresponding States. *J. Chem. Phys.* **1945**, *13*, 253–261.
- (60) Shereshefsky, J. L. Surface Tension of Saturated Vapors and the Equation of Eötvös. *J. Phys. Chem.* **1931**, *35*, 1712–1720.
- (61) Reiss, H.; Mayer, S. W. Theory of the Surface Tension of Molten Salts. *J. Chem. Phys.* **1961**, *34*, 2001–2003.
- (62) Poling, B. E.; Prausnitz, J. M.; O'Connell, J. P. *The Properties of Gases and Liquids*, 5th ed.; McGraw-Hill: New York, 2000.

(63) Rebelo, L. P. N.; Canongia Lopes, J. N.; Esperanca, J. M. S. S.; Filipe, E. On the Critical Temperature, Normal Boiling Point, and Vapor Pressure of Ionic Liquids. *J. Phys. Chem. B* **2005**, *109*, 6040–6043.

(64) Singh, R. K.; Singh, M. P.; Chaurasia, S. K. Temperature Dependent Ultrasonic and Conductivity Studies in Aqueous Polymeric Solution. *Fluid Phase Equilib.* **2009**, *284*, 10–13.

(65) Davila, M. J.; Aparicio, S.; Alcalde, R.; Garcia, B.; Leal, J. M. On the Properties of 1-Butyl-3-methylimidazolium Octylsulfate Ionic Liquid. *Green Chem.* **2007**, *9*, 221–232.

(66) Singh, M. P.; Singh, R. K.; Chandra, S. A New Technique for Determination of Melting Temperature of Poly(Ethylene Glycol) by Ultrasonic Velocimetry. *Phase Transition* **2009**, *82*, 599–506.

(67) Gu, Z.; Brennecke, J. F. Volume Expansivities and Isothermal Compressibilities of Imidazolium and Pyridinium-Based Ionic Liquids. *J. Chem. Eng. Data* **2002**, *47*, 339–345.